Turkish Journal of Electrical Engineering & Computer Sciences

http://journals.tubitak.gov.tr/elektrik/

Research Article

Turk J Elec Eng & Comp Sci
(2018) 26: 856 – 866

doi:10.3906/elk-1606-480

Improved IIR-type fractional order digital integrators using cat swarm optimization

Shibendu MAHATA[1,*], **Suman Kumar SAHA**[2], **Rajib KAR**[1], **Durbadal MANDAL**[1]
[1]Department of Electronics and Communication Engineering, National Institute of Technology, Durgapur, India
[2]Department of Electronics and Telecommunication Engineering, National Institute of Technology, Raipur, India

Received: 29.06.2016 • **Accepted/Published Online:** 24.01.2018 • **Final Version:** 30.03.2018

Abstract: Design of wideband infinite impulse response (IIR) digital fractional order integrators (DFOIs) based on a bio-inspired metaheuristic optimization approach called the cat swarm optimization (CSO) algorithm is presented in this paper. To investigate the efficiency of the proposed approach, the CSO-based DFOIs are evaluated against those of the approximations designed using real-coded genetic algorithm (RGA), standard particle swarm optimization (PSO), and differential evolution (DE) by different magnitude and phase response error metrics. Simulation results reveal the better frequency response of the CSO-based DFOIs in comparison with the competing designs. Both parametric and nonparametric statistical hypothesis tests validate the performance consistency of CSO. Comparisons with the cited literature confirm the efficacy of the proposed models.

Key words: Signal processing, digital fractional order integrators, cat swarm optimization, metaheuristic optimization, statistical tests

1. Introduction

The fractional order integrators and differentiators [1] find applications in several domains [2–4] due to their ability to describe the dynamical behavior of physical systems in an accurate manner [5]. A fractional order integrator (FOI) is a system of infinite dimension and is characterized by the frequency response as given in (1).

$$H_{FOI}(j\omega) = \frac{1}{(j\omega)^p} = \frac{1}{\omega^p}\angle(-90^\circ \times p), \tag{1}$$

where p is the order of the FOI, $p \in (0, 1)$, and ω is the angular frequency.

DFOIs are the digital approximated models for FOIs. In practical applications, DFOIs with smaller orders are preferred since they reduce the computational complexity. Both direct and indirect discretization techniques are used for DFOI design. The direct discretization approach uses the power series expansion [6], continued fraction expansion (CFE) [7,8], Taylor series expansion [9], and MacLaurin series expansion [10], along with operators such as Tustin [11,12], Simpson [13], Al-Alaoui [14], mixed Tustin–Simpson [15], and the impulse response [16]. The least square method [17], Chebyshev–Padé approximation [18], and the rational Chebyshev approximations [18] to design IIR DFOIs have also been reported. In the indirect discretization method [19–21], the frequency domain mapping is performed in the continuous time domain, and the resultant transfer

*Correspondence: shibendu.mahata@gmail.com

function is discretized. In the recent literature, the designs of DFOIs have been reported using discretization of PSO optimized integer order digital integrators (DIs) [22]. PSO optimized DFOIs with an improved magnitude response have also been reported in [23]. Power series expansion-based signal modelling is used to design DFOIs in [24]. It may be noted that while variable DFOIs are reported in [25], however, this work deals with the accurate realization of fixed DFOIs using a bio-inspired optimization algorithm called CSO [26]. While all the DFOI design techniques cited in [6–24] employ a discretization operator, the approach presented in this paper can generate the optimal IIR filter coefficients for the DFOIs without using any such operator. Hence, the novelty of this paper is to present a single-step approach to obtain optimal and highly accurate DFOI models as compared with the multistep DFOI realization methods reported in [6–24].

The rest of the paper is organized as follows: Section 2 provides the DFOI optimization problem formulation. In Section 3, the proposed design problem is addressed using the CSO optimizer. The simulation results, presented in Section 4, are exhaustively compared among the RGA-, PSO-, DE-, and CSO-based DFOIs based on the frequency responses. In addition, two statistical tests are employed to analyze the design robustness of CSO. A comparison with the cited literature is also presented. Finally, the essential conclusions of this work are discussed in Section 5.

2. Problem formulation

The transfer function of the IIR DFOI of order N is defined by (2).

$$H(z) = \frac{a_1 + a_2 z^{-1} + a_3 z^{-2} + ... + a_{N+1} z^{-N}}{b_1 + b_2 z^{-1} + b_3 z^{-2} + ... + b_{N+1} z^{-N}}, \tag{2}$$

where a_i and b_i, $i = 1, 2, 3, ..., N+1$, represent the numerator and denominator coefficients, respectively, of $H(z)$.

In this work, RGA [27], PSO [28], DE [29], and CSO algorithm [26] individually determine the optimal values of coefficients of $H(z)$ such that the root mean square magnitude error (RMSME) as given by (3) is minimized.

$$RMSME = \sqrt{\frac{\sum ||H_{FOI}(\omega)| - |H(\omega)||^2}{q}} \tag{3}$$

Here q denotes the total sampled data points spaced between 0.02π to π radians/second.

The error metrics used for performance comparison among the DFOIs are the maximum absolute relative magnitude error (MARME) and the absolute magnitude error (AME) as defined by (4) and (5), respectively.

$$MARME = Max\{\left|\frac{|H_{FOI}(\omega)| - |H(\omega)|}{|H_{FOI}(\omega)|}\right|\} \tag{4}$$

$$AME = ||H(\omega)| - |H_{FOI}(\omega)|| \tag{5}$$

The group delay of the IIR DFOI is given by (6).

$$\tau = -\frac{d\theta(\omega)}{d\omega}, \tag{6}$$

where $\theta(\omega) = \angle H(\omega)$ is the phase angle of the DFOI.

It is worth emphasizing that while the CSO algorithm has been employed for the identification of a few well-known benchmark IIR plants in [30], this paper presents the design of IIR DFOIs using CSO for the first time in the literature. Furthermore, unlike [30], a thorough analysis based on the magnitude and phase responses of the designed DFOI model-based signal processing system is investigated. Additionally, while [30] employs a white signal of zero mean, unit variance, and uniform distribution for the system identification technique, the proposed optimization method is carried out entirely in the frequency domain as defined by (3).

3. Cat swarm optimization (CSO) algorithm

CSO is a metaheuristic optimization algorithm inspired by the optimal use of body energy by cats [26]. The search strategy in CSO is based on employing the cats to function in two different modes, namely the seeking mode and the tracing mode. Each randomly initialized n_p number of cats in the $D = (N+1) \times 2$ dimensional problem search space has its position, velocity, an error fitness value, and a flag to determine if it is in seeking mode or in tracing mode. The ratio of the total quantity of cats present in the tracing mode concerning the entire population of cats in the DFOI design problem search space is called the mixture ratio (MR). MR provides a balance between diversification and intensification phases in CSO. The optimal solution in CSO is the best position attained by any one of the cats. The two modes of operation of CSO are as follows.

3.1. Seeking mode

The seeking mode models the resting but the alert behavior of a cat. Hence, this mode deals with the process of diversification in the DFOI design problem search space. The control parameters used in this mode are defined as follows.

Seeking memory pool (SMP): The total number of copies of a cat generated in the seeking mode.

Seeking range of selected dimension (SRD): The maximum difference that exists between the present and the past values in the dimension that is selected to undergo mutation.

Counts of dimension to change (CDC): The total number of dimensions to undergo mutation.

The following steps are employed in the seeking mode:

Step 1. From a randomly generated population of n_p $(= 50)$ number of cats, randomly select MR fraction of cats in the tracing mode and $(1 - MR)$ fraction of cats in the seeking mode.

Step 2. Create SMP number of copies for the ith cat in the seeking mode.

Step 3. Depending on the value of CDC, the positions of all the copies are updated by conducting random addition or subtraction of SRD fraction of the current value of the position.

Step 4. Determine the error fitness value for all the copies according to (3).

Step 5. Identify the cat with the least value of error fitness and place it at the location of an ith cat in the seeking mode.

Step 6. Repeat from Step 2 until all the cats are exhausted.

3.2. Tracing mode

This mode deals with the intensification phase in the optimization problem search space. This mode models the tracing of prey by a cat, which results in a considerable expenditure of its body energy. Hunting the prey by the cat is modelled regarding a substantial change in its position. The position and the velocity for the ith

cat are defined by (7) and (8), respectively.

$$X_i = (X_{i1},\, X_{i2},\, ...,\, X_{iD}) \tag{7}$$

$$V_i = (V_{i1},\, V_{i2},\, ...,\, V_{iD}), \tag{8}$$

where D is the dimension of the optimization problem.

The global best position *gbest* of the population of cats is modelled by (9).

$$gbest = (gbest_1,\, gbest_2,\, ...,\, gbest_D) \tag{9}$$

The velocity and the position of the ith cat are given by (10) and (11), respectively.

$$V_{iD} = w \times V_{iD} + C \times m \times (gbest_D - X_{iD}), \tag{10}$$

where w represents the inertia weight; C denotes the acceleration constant; $m \in [0,\, 1]$ is a random number with uniform distribution.

$$X_{iD} = X_{iD} + V_{iD} \tag{11}$$

Figure 1 shows the flowchart of the CSO algorithm.

4. Simulation results and discussion

RGA [27], PSO [28], and DE [29] are popular evolutionary optimization algorithms and are not examined here. However, the chromosome representation of RGA for DFOI design based on the two-point crossover technique is shown in Figure 2. In this work, the two-point crossover is used for RGA where the two cut points are randomly generated. While choosing more than two cut-points increases the optimization time for RGA, a single-point crossover is too simple. Hence, the two-point crossover is preferred in this work.

The values of the parameters of the benchmark algorithms and CSO selected for this work are presented in Table 1. The designed DFOIs of orders 3 and 5 based on RGA, PSO, DE, and CSO achieved by minimizing (3) by setting p = 0.50 are shown in (12)–(19).

$$H_{RGA\_3}(z) = \frac{0.9381 - 0.9511z^{-1} + 0.0869z^{-2} + 0.0505z^{-3}}{0.9976 - 1.5956z^{-1} + 0.6229z^{-2} - 0.0044z^{-3}} \tag{12}$$

$$H_{PSO\_3}(z) = \frac{0.9155 - 0.9423z^{-1} + 0.0866z^{-2} + 0.0572z^{-3}}{0.9832 - 1.5893z^{-1} + 0.6359z^{-2} - 0.0109z^{-3}} \tag{13}$$

$$H_{DE\_3}(z) = \frac{0.9411 - 0.9376z^{-1} + 0.0926z^{-2} + 0.0518z^{-3}}{1.0111 - 1.5947z^{-1} + 0.6368z^{-2} - 0.0217z^{-3}} \tag{14}$$

$$H_{CSO\_3}(z) = \frac{0.9400 - 0.9197z^{-1} + 0.0521z^{-2} + 0.0563z^{-3}}{1.0170 - 1.5760z^{-1} + 0.5726z^{-2} + 0.0123z^{-3}} \tag{15}$$

$$H_{RGA\_5}(z) = \frac{0.9597 + 0.0871z^{-1} - 0.6719z^{-2} - 0.0914z^{-3} + 0.1169z^{-4} - 0.0268z^{-5}}{1.0397 - 0.5055z^{-1} - 0.8463z^{-2} + 0.2425z^{-3} + 0.2146z^{-4} - 0.0780z^{-5}} \tag{16}$$

$$H_{PSO\_5}(z) = \frac{0.9623 + 0.0934z^{-1} - 0.6780z^{-2} - 0.0868z^{-3} + 0.1385z^{-4} - 0.0277z^{-5}}{1.0446 - 0.4971z^{-1} - 0.8559z^{-2} + 0.2436z^{-3} + 0.2355z^{-4} - 0.0893z^{-5}} \tag{17}$$

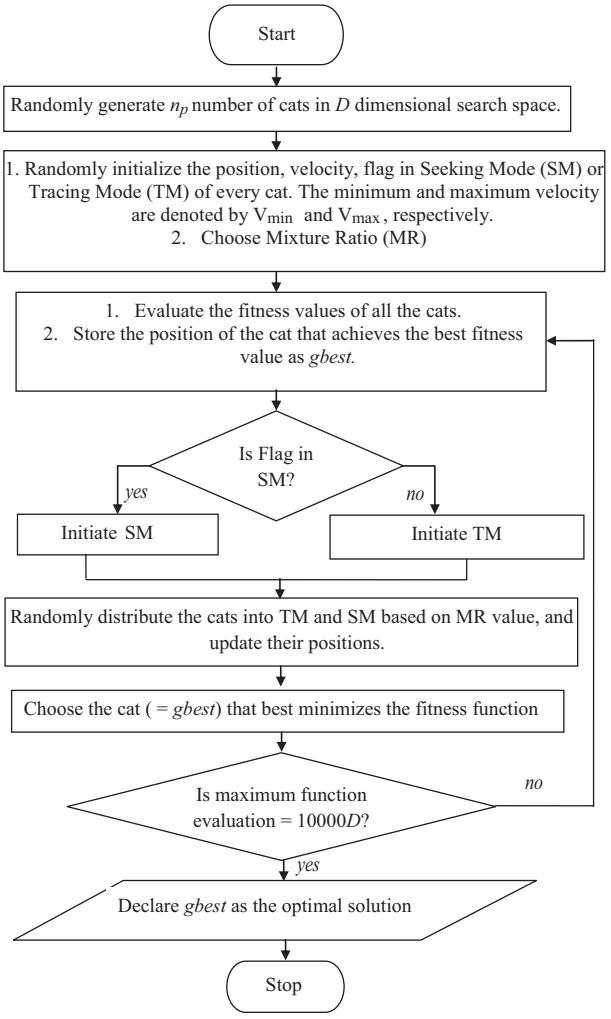

Figure 1. Flowchart of CSO.

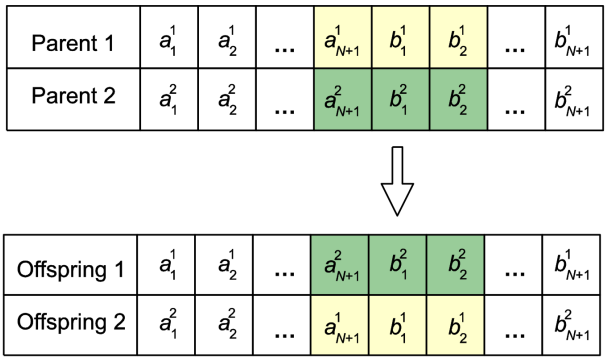

Figure 2. Chromosome representation for RGA-based DFOI design.

$$H_{DE\_5}(z) = \frac{0.9642 + 0.0936z^{-1} - 0.6663z^{-2} - 0.0851z^{-3} + 0.1182z^{-4} - 0.0333z^{-5}}{1.0577 - 0.4941z^{-1} - 0.8669z^{-2} + 0.2452z^{-3} + 0.2253z^{-4} - 0.0840z^{-5}} \tag{18}$$

Table 1. Parameter values of the algorithms used in this work.

Parameter	RGA	PSO	DE	CSO
Size of population	50	50	50	50
Maximum number of function evaluations	10,000 $\times D$	10,000 $\times D$	10,000 $\times D$	10,000 $\times D$
Crossover probability, crossover	0.80, Two point	-	-	-
Mutation probability, mutation	0.01, Gaussian (mean : 0, variance : 1)	-	-	-
Selection, elitism	Roulette wheel, 1 / 5	-	-	-
C_1, C_2	-	1.494, 1.494	-	-
$\left\|v_i^{\min}\right\|, \left\|v_i^{\max}\right\|$	-	0.01, 1.0	-	-
$w_{\max}$, w_{min}	-	0.9, 0.4	-	-
C_r, F	-	-	0.5, 0.05	-
SMP, *CDC*, *SRD*	-	-	-	5, 0.6, 2
MR	-	-	-	0.1
w, C	-	-	-	0.4, 1.5
V_{min}, $V_{\max}$	-	-	-	- 0.1, 0.1

$$H_{CSO\_5}(z) = \frac{0.9480 - 1.6230z^{-1} + 0.7107z^{-2} + 0.0104z^{-3} - 0.0354z^{-4} + 0.0074z^{-5}}{1.0220 - 2.3480z^{-1} + 1.7380z^{-2} - 0.4259z^{-3} + 0.0213z^{-4} - 0.0057z^{-5}} \tag{19}$$

5. Comparison of frequency response

Table 2 confirms that CSO-based DFOIs outperform the competing DFOIs by RMSME and MARME metrics. The CSO-based designs also demonstrate the least sample deviation from the flat group delay ($\tau_{\max}$). Figures 3(a)–(f) present the magnitude, AME, and phase plots of the designs, respectively.

Table 2. Comparison among the designed DFOIs.

N	Algorithm	RMSME (dB)	MARME (dB)	$\tau_{\max}$ (samples)
3	RGA	–24.6	–19.1	5.11
	PSO	–26.3	–19.8	5.07
	DE	–29.6	–20.1	5.24
	CSO	–42.0	–27.9	4.47
5	RGA	–30.4	–25.1	5.38
	PSO	–32.5	–26.7	5.52
	DE	–33.7	–26.9	5.17
	CSO	–39.5	–30.8	0.47

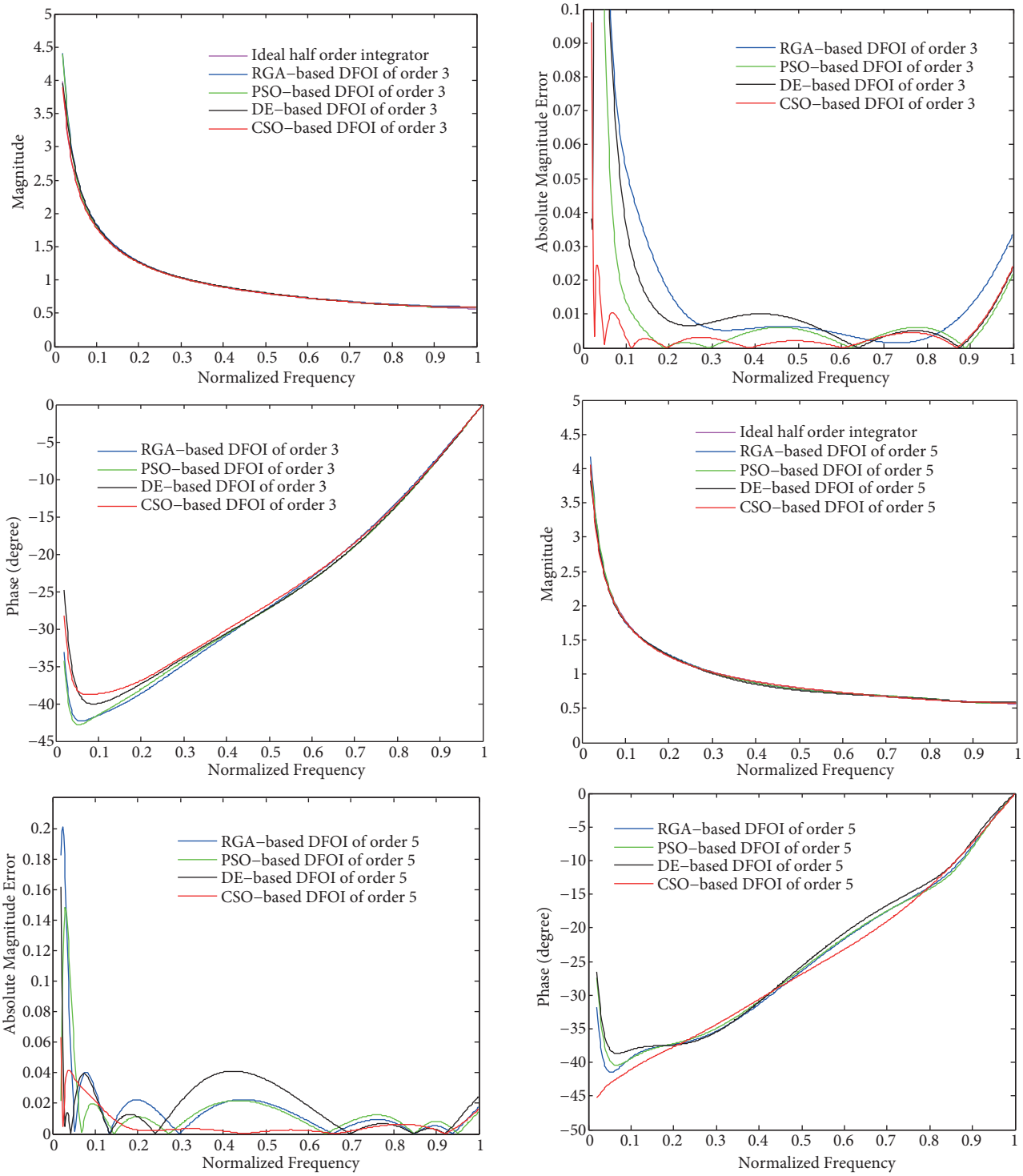

Figure 3. (a) Magnitude responses of the designed DFOIs of order 3. (b) AME responses of the designed DFOIs of order 3. (c) Phase responses of the designed DFOIs of order 3. (d) Magnitude responses of the designed DFOIs of order 5. (e) AME responses of the designed DFOIs of order 5. (f) Phase responses of the designed DFOIs of order 5.

5.1. Consistency analysis

The performance of CSO as a consistently accurate optimizer for the design of DFOIs is statistically confirmed by conducting the t-test [31] and the Wilcoxon rank-sum test [31] on RGA-CSO, PSO-CSO, and DE-CSO pairs. These pair-wise statistical procedures perform individual comparisons between two algorithms, obtaining in each application a P-value independent from one another. Thus, to carry out a comparison that involves more than two algorithms, multiple comparison tests are used. The testing of the null hypothesis statement where both the data samples are gathered from a population with identical mean and having normal distribution is performed by conducting the two sample t-test. This parametric type hypothesis test assumes independence, normality, and homoscedasticity of data samples. On the other hand, the Wilcoxon rank-sum test is a nonparametric hypothesis test that tests the similarity or dissimilarity in the performance of the algorithms/approaches/applications based on two data sets gathered from the same population without conforming to a particular type of data distribution. Thus, the Wilcoxon test does not assume the properties of independence, normality, and homoscedasticity. These hypothesis tests can be conducted at a fixed level of significance, α, or by determining the smallest level of significance (called P-value) that results in the rejection of the null hypothesis. Thus, the smaller the P-value, the higher is the evidence to reject the null hypothesis.

In this work, the null hypothesis statement for these tests (at 99% significance) is defined as: "RMSME performance for the designed DFOIs does not show any significant difference". Both the tests are performed with 60 data samples from each algorithm and for each order of DFOI. These data samples are generated by executing the RGA-, PSO-, DE-, and CSO-based optimization programs written in MATLAB programming language for 60 independent trial runs for each of the algorithms for both the orders of the DFOIs. Tables 3 and 4 show the t-test and the rank-sum test results, respectively. The decision for the test is given by h = 1/0 for the rejection/acceptance of the null hypothesis. The confidence interval for the t-test result is denoted by CI. Both the tests show an h-index of 1, which proves that there is a significant difference in the performance of the designed DFOIs based on CSO as compared with RGA/PSO. That is, CSO provides significantly accurate DFOI models as compared with those designed with the other algorithms. A very small P-value is also obtained for each of the design cases for both these tests as shown in Tables 3 and 4. Hence, the results obtained for both the tests reveal that CSO-based designs consistently outperform the competing DFOIs by achieving the smallest RMSME for all the test cases. Thus, CSO can be regarded as a consistently superior optimization tool for realizing IIR DFOIs.

Table 3. t-test results.

N	Index	Algorithm pair		
		CSO/RGA	CSO/PSO	CSO/DE
3	h	1	1	1
	P-value	6.17×10^{-51}	1.27×10^{-51}	1.40×10^{-43}
	CI	[–22.3, –18.3]	[–19.4, –15.9]	[–15.5, –12.2]
5	h	1	1	1
	P-value	7.49×10^{-34}	1.27×10^{-25}	1.86×10^{-21}
	CI	[–14.5, –10.6]	[–10.2, –6.9]	[–8.3, –5.3]

Table 4. Wilcoxon rank-sum test results.

N	Index	Algorithm pair		
		CSO/RGA	CSO/PSO	CSO/DE
3	h	1	1	1
	P-value	3.55×10^{-21}	3.73×10^{-21}	5.04×10^{-21}
5	h	1	1	1
	P-value	8.72×10^{-20}	3.17×10^{-18}	5.92×10^{-16}

5.2. Comparison with the literature

Table 5 shows the evaluation of RMSME and MARME performances of the proposed CSO-based DFOIs with the cited literature. It is easily seen that both the error metrics are significantly smaller for the proposed DFOIs. Figures 4(a) and 4(b) show the AME plots for the CSO-based DFOIs along with the reported designs, which justify the improved modelling accuracy of the proposed designs.

Table 5. Comparison of proposed DFOIs with the cited literature.

N	Model	RMSME	MARME
		(decibel)	(decibel)
3	(2013) [22] PSO	–17.7	–11.5
	(2015) [23] PSO	–15.1	–9.6
	(2015) [23] Linear interpolation	–16.9	–10.3
	CSO	–42.0	–27.9
5	(2013) [18] Chebyshev–Padé with Tustin	–23.2	–9.3
	(2015) [20] Indirect discretization	–33.2	–25.1
	(2015) [23] Linear interpolation	–23.6	–15.9
	(2015) [23] PSO	–24.9	–17.0
	(2015) [24] Power series expansion series modelling	–26.1	–15.5
	CSO	–39.5	–30.8

6. Conclusions

This paper presents a population-based bio-inspired optimization algorithm called CSO for the efficient design of accurate digital fractional order integrators (DFOIs). The research work (a) demonstrates the applicability of the CSO algorithm for the design of stable and accurate wideband DFOIs, and (b) justifies the superiority of CSO-based DFOIs over the designs based on RGA, PSO, DE, and the published literature with respect to different performance indices. Both parametric and nonparametric hypothesis tests results statistically validate that CSO-based DFOIs consistently outperform the competing designs and attain the smallest RMSME. The CSO-based third and fifth order designs also demonstrate improvements in RMSME of 137.28% and 18.97%, respectively, over the best approximations cited in the literature.

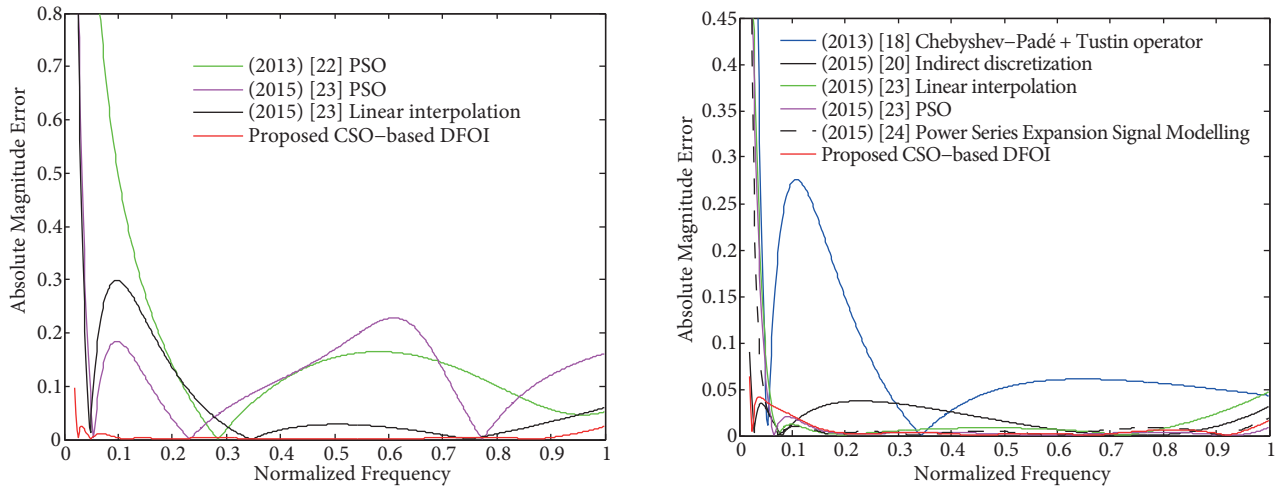

Figure 4. (a) AME plot comparison for the proposed CSO-based DFOIs ($N = 3$) with the reported designs. (b) AME plot comparison for the proposed CSO-based DFOIs ($N = 5$) with the reported designs.

Acknowledgment

The financial support to conduct this research is provided by Visvesvaraya Young Faculty Fellowship, MeitY, Govt. of India (Grant No. PhD-MLA-4(29)/ 2015-16).

References

[1] Oldham KB, Spanier J. The Fractional Calculus. New York, NY, USA: Academic Press, 1974.

[2] Podlubny I. Fractional-order systems and PI$^{\lambda}$D$^{\mu}$ –controllers. IEEE T Automat Contr 1999, 44: 208-214.

[3] Vinagre BM, Monje CA, Calderon AJ, Suarez JI. Fractional PID controllers for industry applications – a brief introduction. J Vib Control 2007; 13: 1419-1429.

[4] Yeroglu C, Tan N. Classical controller design techniques for fractional order case. ISA T 2011; 50: 461-472.

[5] West BJ, Bologna M, Grigolini P. Physics of fractal operators. 1st ed. New York, NY, USA: Springer Verlag, 2003.

[6] Ferdi Y. Computation of fractional order derivative and integral via power series expansion and signal modelling. Nonlinear Dynam 2006; 46: 1-15.

[7] Chen YQ, Vinagre BM, Podlubny I. Continued fraction expansion approaches to discretizing fractional order derivatives - an expository review. Nonlinear Dynam 2004; 38: 155-170.

[8] Maione G. Closed-form rational approximations of fractional, analog and digital differentiators/integrators. IEEE J Em Sel Top C 2013; 3: 322-329.

[9] Gupta M, Varshney P, Visweswaran GS. Digital fractional-order differentiator and integrator models based on first-order and higher order operators. Int J Circ Theor App 2011; 39: 461-474.

[10] Valerio D, Costa JS. Time-domain implementation of fractional order controllers. IEE P-Contr Theor Ap 2005; 152: 539-552.

[11] Vinagre BM, Chen YQ, Petras I. Two direct Tustin discretization methods for fractional-order differentiator/integrator. J Frankl Inst 2003; 340: 349-362.

[12] Vinagre BM, Podlubny I, Hernandez A, Feliu V. Some approximations of fractional order operators used in control theory and applications. Fract Calc Appl Anal 2000; 3: 231-248.

[13] Tseng CC. Design of FIR and IIR fractional order Simpson digital integrators. Signal Process 2007; 87: 1045-1057.

[14] Chen YQ, Moore KL. Discretization schemes for fractional-order differentiators and integrators. IEEE T Circuits Syst-I: Fundam Theory A 2002; 49: 363-367.

[15] Chen YQ, Vinagre BM. A new IIR-type digital fractional order differentiator. Signal Process 2003; 83: 2359-2365.

[16] Maione G. Continued fractions approximation of the impulse response of fractional-order dynamic systems. IET Control Theory A 2008; 2: 564-572.

[17] Barbosa RS, Machado JAT, Silva MF. Time domain design of fractional differintegrators using least-squares. Signal Process 2006; 86: 2567-2581.

[18] Romero M, de Madrid AP, Manoso C, Vinagre BM. IIR approximations to the fractional differentiator/integrator using Chebyshev polynomials theory. ISA T 2013; 52: 461-468.

[19] Krishna BT. Studies of fractional order differentiators and integrators: a survey. Signal Process 2011; 91: 386-426.

[20] Yadav R, Gupta M. Approximations of higher-order fractional differentiators and integrators using indirect discretization. Turk J Electr Eng & Comp Sci 2015; 23: 666-680.

[21] Gupta M, Yadav R. Design of improved fractional order integrators using indirect discretization method. Int J Comput Appl 2012; 59: 19-24.

[22] Gupta M, Yadav R. Optimization of integer order integrators for deriving improved models of their fractional counterparts. J Optimiz 2013; 2013: article id. 142390.

[23] Yadav R, Gupta M. New improved fractional order integrators using PSO optimization. Int J Electron 2015; 102: 490-499.

[24] Leulmi F, Ferdi Y. Improved digital rational approximation of the operator s^{α} using second-order s-to-z transform and signal modeling. Circ Syst Signal Pr 2015; 34: 1869-1891.

[25] Tseng CC. Designs of discrete-time generalized fractional order differentiator, integrator and Hilbert transformer. IEEE T Circuits-I 2015; 62: 1582-1590.

[26] Chu S, Tsai F. Computational intelligence based on the behaviour of cats. Int J Innov Comput I 2007; 3: 163-173.

[27] Goldberg DB. Genetic algorithms in search optimization and machine learning. San Francisco, CA, USA: Addison-Wesley, 1989.

[28] Kennedy J, Eberhart R. Particle swarm optimization. In: IEEE 1995 International Conference on Neural Networks; 27 November–1 December 1995; Perth, Australia: IEEE. pp. 1942-1948.

[29] Storn R, Price K. Differential evolution - a simple and efficient heuristic for global optimization over continuous spaces. J Global Optim 1997; 11: 341-359.

[30] Panda G, Pradhan PM, Majhi B. IIR system identification using cat swarm optimization. Expert Syst Appl 2011; 38: 12671-12683.

[31] Montgomery DC, Runger GC. Applied Statistics and Probability for Engineers. 3rd ed. Hoboken, NJ, USA: John Wiley and Sons, Inc., 2003.